Brain Stimulation (2011) 4, 169–74

ELSEVIER

BRAIN
STIMULATION

www.brainstimjrnl.com

Individualized model predicts brain current flow during transcranial direct-current stimulation treatment in responsive stroke patient

Abhishek Datta,[a] Julie M. Baker,[b] Marom Bikson,[a] Julius Fridriksson[b]

[a]*Department of Biomedical Engineering, The City College of the New York, City University of New York, New York, New York*
[b]*Department of Communication Sciences and Disorders, University of South Carolina, Columbia, South Carolina*

Although numerous published reports have demonstrated the beneficial effects of transcranial direct-current stimulation (tDCS) on task performance, fundamental questions remain regarding the optimal electrode configuration on the scalp. Moreover, it is expected that lesioned brain tissue will influence current flow and should therefore be considered (and perhaps leveraged) in the design of individualized tDCS therapies for stroke. The current report demonstrates how different electrode configurations influence the flow of electrical current through brain tissue in a patient who responded positively to a tDCS treatment targeting aphasia. The patient, a 60-year-old man, sustained a left hemisphere ischemic stroke (lesion size = 87.42 mL) 64 months before his participation. In this study, we present results from the first high-resolution (1 mm^3) model of tDCS in a brain with considerable stroke-related damage; the model was individualized for the patient who received anodal tDCS to his left frontal cortex with the reference cathode electrode placed on his right shoulder. We modeled the resulting brain current flow and also considered three additional reference electrode positions: right mastoid, right orbitofrontal cortex, and a "mirror" configuration with the anode over the undamaged right cortex. Our results demonstrate the profound effect of lesioned tissue on resulting current flow and the ability to modulate current pattern through the brain, including perilesional regions, through electrode montage design. The complexity of brain current flow modulation by detailed normal and pathologic anatomy suggest: (1) That computational models are critical for the rational interpretation and design of individualized tDCS stroke-therapy; and (2) These models must accurately reproduce head anatomy as shown here.

Keywords tDCS; electrical brain stimulation; human head model; electric fields; aphasia

Transcranial direct-current stimulation (tDCS) is a noninvasive and safe technique designed for modulating cortical activity through the delivery of a weak polarizing electrical current via electrodes placed on the scalp.[1] tDCS has been evaluated to modulate cognitive, linguistic, and motor performance in both healthy and neurologically impaired individuals with results supporting the feasibility of leveraging interactions between stimulation-induced neuromodulation

This work was supported by the following grants: S06GM008168 (PI: M.B.) and NS054783 (PI: M.B.); DC008355 (PI: J.F.) and DC009571 (PI: J.F.).
Correspondence: Abhishek Datta, PhD, Neural Engineering Laboratory, Department of Biomedical Engineering, The City College of New York of CUNY, New York, NY 10031.
E-mail address: abhishek.datta@gmail.com
Submitted July 23, 2010; revised November 8, 2010. Accepted for publication November 9, 2010.

1935-861X/$ - see front matter © 2011 Elsevier Inc. All rights reserved.
doi:10.1016/j.brs.2010.11.001

and task execution.[2-4] For instance, we recently demonstrated that the application of anodal tDCS (A-tDCS) to the left frontal cortex significantly enhanced the effect of aphasia treatment in chronic stroke.[5]

Electrode montage (i.e., the position and size of electrodes) determines the resulting brain current flow and, as a result, neurophysiologic effects. The ability to customize tDCS treatment through electrode montage provides clinical flexibility and the potential to individualize therapies.[6] However, although numerous reports have been published in recent years demonstrating the effects of tDCS on task performance, there remain fundamental questions about the optimal design of electrode configurations. Moreover, it is expected that lesioned tissue will influence current flow,[7] and should therefore be considered in the design of individualized tDCS therapies for stroke.

Computational models using finite element methods (FEM) are standard tools for predicting current flow through the brain during tDCS, and thus have the potential to inform therapeutic strategies. In this study, we present results from the first high-resolution (1 mm^3) model of tDCS in a brain with lesioned tissue; the model was individualized to the patient who participated in our aforementioned chronic stroke tDCS study[5] and was classified as a responder to the tDCS treatment condition as compared with the sham treatment condition. The patient received A-tDCS to his left frontal cortex (Broadmann area [BA] 6) with the reference cathode electrode placed on the right shoulder. In this study, we model the resulting brain current flow and consider three additional electrode configurations: right mastoid, right orbitofrontal cortex, and the mirror of the experimentally used montage.

Materials and methods

Clinical summary

A 60-year-old man sustained a left hemisphere ischemic stroke 64 months before his participation in our tDCS study.[5] He suffered damage to BA 44, BA 45, BA 38, as well as the middle and anterior insula (lesion size = 87.42 mL). According to the *Western Aphasia Battery-Revised*,[8] the patient's language deficits are most consistent with Broca's aphasia. He received 5 days of A-tDCS (1 mA; 20 minutes) and 5 days of sham tDCS (S-tDCS; 20 minutes), while performing a computerized anomia treatment and was classified as one of the best responder's in the study (reference [5] for additional specific study details).

Magnetic resonance imaging-derived high-resolution model

The individualized head model was created from 1 mm^3 resolution T1-weighted and T2-weighted magnetic resonance imaging (MRI) scans of the patient collected using a 3 T Siemens Trio scanner (Erlangen, Germany) with a 12-element head coil. A combination of automated and manual segmentation tools were used to obtain the tissue masks. Automatic segmentation was performed using FSL from the Functional MRI of the Brain (FMRIB) Software Library (London, UK). FSL Brain Extraction Tool (BET) and FSL Automated Segmentation Toolbox (FAST) were used to segment the MRI data into scalp, skull, cerebrospinal fluid (CSF), gray matter, and white matter.[9] Typically automatic head/brain segmentation tools such as FSL are optimized to accurately distinguish brain tissue masks from nonbrain tissue masks, and segmentation errors are introduced in other tissue masks. Some of these errors are due to: (1) skull producing low signals in MRI and it is thus difficult to distinguish from surrounding layers; (2) skull and air have overlapping intensity; (3) difficulties in demarcating lesion site boundaries; and (4) artifactual discontinuities for thin tissues such as CSF (http://www.neuralengr.com/modelmethods). Therefore, manual correction was necessary to correct for the automatic segmentation errors. Using a combination of segmentation tools (Point to Point line, Smoothing filters and Boolean operations) from ScanIP (Simpleware Ltd, Exeter, UK), automated segmentation masks were corrected and the data were further segmented into compartments representing eye region, muscle, air, and blood vessels (Custom Segmentation, Soterix Medical, New York, NY; Figure 1). The lesion site was classified as CSF as shown by both imaging and histopathology studies.[7,10,11] The stimulation electrodes/sponges were physically rendered as CAD files (.STL) and positioned on the segmented head using ScanCAD (Simpleware Ltd).

The finite element (FE) adaptive mesh generated from the segmentation and CAD masks (minimum quality factor: 0.4) was exported to COMSOL Multiphysics 3.5a (Burlington, MA) for computation of electric fields.[12] The model comprised $>$ 10 million elements with $>$ 15 million degrees of freedom.

Model solution

We modeled four electrode configurations: (1) right shoulder, (2) right mastoid, (3) right orbitofrontal cortex, and (4) mirror right shoulder (Figure 1). Because the head model was directly derived from previously collected MRI data, it was limited to the anatomic sections collected.[13] Thus, to model the extracephalic clinical montage used in our aforementioned tDCS study,[5] a synthetic neck and shoulder region was fused onto the existing segmented head. The stimulation electrodes were modeled as 5 $\times$ 5 cm sponge-based electrodes and current densities corresponding to 1 mA total current were applied at the anode electrode.[5,12] Ground was applied at the negative electrode and all other external surfaces were treated as insulated.

The following isotropic electrical conductivities (in S/m) were assigned: gray matter: 0.276; white matter: 0.126; CSF: 1.65; skull: 0.01; scalp: 0.465; eye region: 0.4; air: 1e-

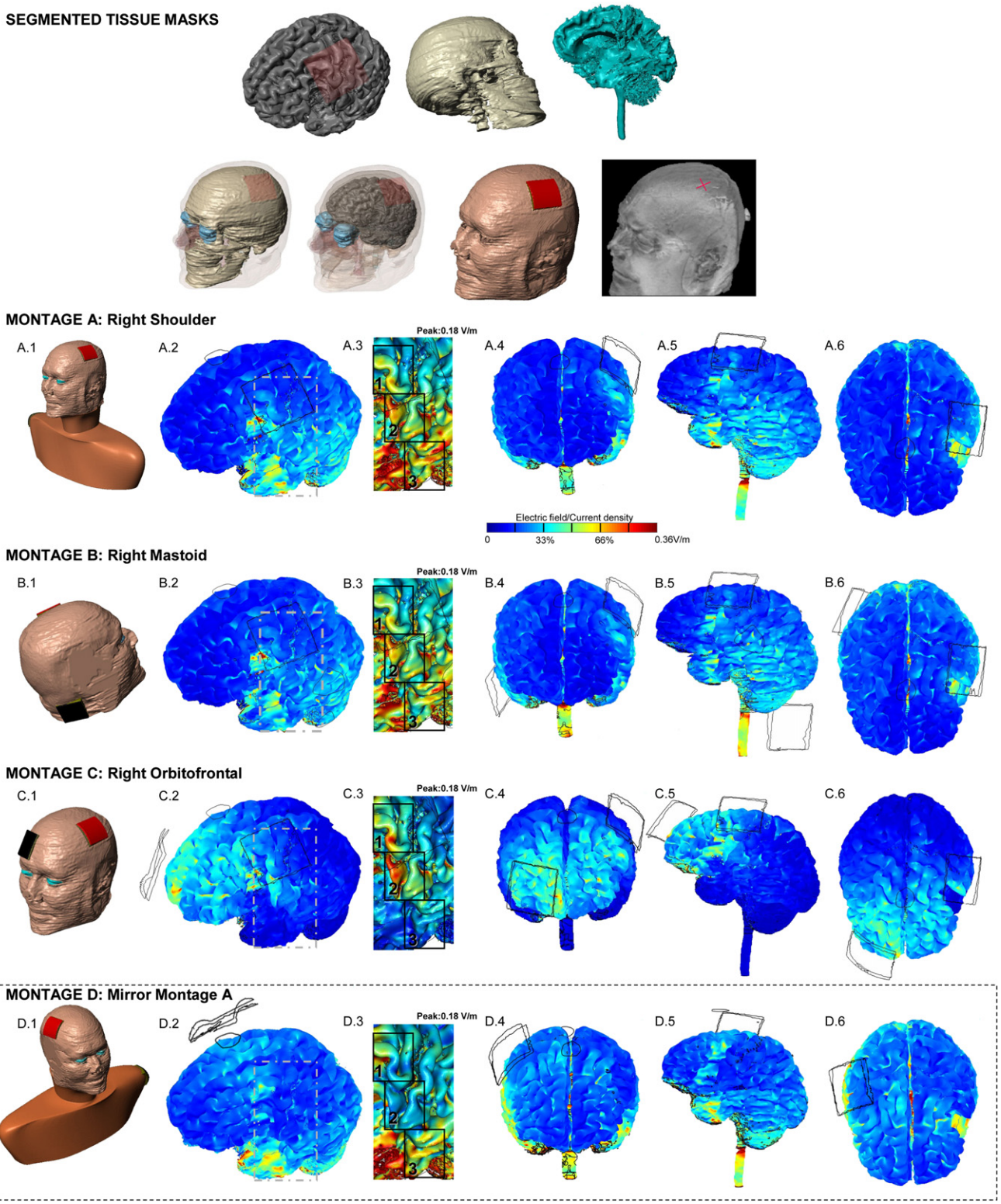

Figure 1 Computational results of cortical currents during tDCS using a 1 mm^3 resolution patient-specific head model. The top two rows show sample segmentation masks. First: gray matter, skull, white matter. Juxtaposed images of the FE model (rendered from the segmentation masks) and 3-dimensional model (rendered from patient's MRI scans using MRIcro) are also shown. All the images in the second row are plotted with the same view. **Montage A**: right shoulder; **Montage B**: right mastoid; **Montage C**: right orbitofrontal; **Montage D**: mirror Montage A. All false color maps were generated between 0 and 0.36 V/m; the *peak* cortical electric field (EF) magnitude for Montage A. Surface magnitude plots of EF were generated with different views. **A.2, B.2, C.2,** and **D.2** show current flow in the *lesional* and *perilesional* areas. The dashed region is expanded in **A.3, B.3, C.3,** and **D.3** and scaled between 0 and 0.18 V/m (half of the *peak* EF for Montage A) to highlight current flow in the *posterior perilesional* areas. **A.4**, **B.4**, **C.4,** and **D.4**: Frontal view. **A.5**, **B.5**, **C.5,** and **D.5**: left side view. **A.6**, **B.6, C.6,** and **D.6:** top view.

15; synthetic region: 0.35; sponge: 1.4; electrode: 5.8e7.[7,12] The muscle and blood vessel compartments were assigned the conductivity of scalp tissue. The Laplace equation was solved and the linear system iterative solver of conjugate gradients (with a relative tolerance of 1×10^{-6}) was used.[12,14] Cortical electric field (EF) surface and cross-section magnitude maps for the different electrode montages were determined (Figures 1 and 2).[12] EF/current density magnitude is commonly used to predict neuronal modulation in transcranial stimulation modeling.[7,12,15,16] For weak static fields, neuronal excitability changes monotonically with strength of EF magnitude[17,18] (see discussion in reference[14]).

Results

The current flow pattern through the brain during tDCS was modulated by the presence of the lesion (Figures 1 and 2) as compared with a healthy head.[12] Manifest changes in the resulting cortical EFs were observed in both the perilesional regions and wider cortical regions. The relatively conductive lesion concentrated current in the perilesional area, especially in deep brain regions between stimulation electrodes (Figure 1, A.3, B.3, C.3, D.3). As in the healthy head,[12] the overall current pattern was complex, reflecting the overall detailed neuroanatomy and convoluted cortical topography. For example, the highly conductive ventricles resulted in a preferential current flow reflected in surrounding brain regions; together with the lesioned region forming a highly attractive current path. The modulation of current flow by the lesioned region was pronounced even when both electrodes were placed away from the lesion (Montage D, see below).

The position of the reference cathode affected brain current flow and resulting EFs both in the perilesional and wider cortical lesions. With an orbitofrontal cathode, current flow was most restricted to the upper hemispheres, with substantial EFs in the cortex under the cathode and in frontal regions between the electrodes (Figure 1, C). Positioning of the cathode on the contralateral shoulder (Figure 1, A) or on the contralateral mastoid (Figure 1, B), increased the current flow in the temporal lobes and brainstem—consistent with an overall preferred current flow down the ispsilateral side of the head, through the lesion, across the ventral perilesional regions, through foramen magnum, and then to the return cathode on contralateral side (Figure 2, A.2, A.3, B.2, B.3). The right shoulder montage resulted in the highest and the most widespread EFs in the posterior perilesional cortex (in the cortex roughly under the anode), although the orbitofrontal cathode montage produced the highest electric field in cortical region anterior to the lesion, including anterior perilesional cortex.

The mirror montage (Montage D) led to considerable current flow in the right hemisphere underneath the stimulation pad, as expected (Figure 2, D.3, D.4, D.5). However, the presence of the lesion also led to current flow being funneled across from the upper right to upper left hemispheres into the infarction site.

The importance of detailed cortical and lesioned anatomy is highlighted by consideration of the three demarcated regions (1-3) in the posterior perilesional cortex (Figure 1, A.3, B.3, C.3, D.3). The EF distribution is clearly shaped by and follows the contours of the cortical surface. Montage A produced the highest average and widespread EFs across these regions, whereas Montage B resulted in slightly less stimulation most notably in region 3. Thus, even moving the return cathode from the contralateral mastoid to the contralateral shoulder results in (moderate) changes in current flow under the active anode. Montage C produced the highest EF in region 1, whereas region 3 was largely spared. Montage D, with neither an active or return electrode over the perilesional region, resulted in increased current flow over region 3 (even more so than Montage C). This specific analysis also serves to exemplify an important insight: that analysis of the role of electrode montage must be guided by precise consideration of (complex) current flow, which neither "coarse" models (e.g., spheres), generic metrics, nor clinical intuition will capture.

Discussion

If tDCS continues to be revealed as a viable option for treatment in chronic stroke, the consideration of tDCS-generated current flow through the brain is of fundamental importance for the identification of candidates, optimization of electrotherapies for specific brain targets, and interpretation of patient-specific results—thus the ability to individualize tDCS therapy must be leveraged. Whereas, tDCS electrode montages are commonly designed using "gross" intuitive rules (e.g., anode positioned "over" the target region), our results reinforce the complexity of current flow, including the critical importance of "return" electrode positioning,[19] and thus the value of applying predictive modeling as one tool in the rational design of safe and effective electrotherapies. Moreover, our results support the value of individualized models and therapy design because of the profound effect of cortical damage on overall current flow.

Our high-resolution individualized tDCS model predicts current flow (EF) through each brain region. Though it is rational to speculate that those regions with higher EFs will be more likely candidates for brain modulation—and thus electrode montages should be selected to maximize currents in "target" regions—there remain fundamental unknowns about both the neurophysiology of prolonged weak DC stimulation and the processes of stroke recovery. There are indeed competing or complementary views of optimal brain activation/deactivation to facilitate stroke

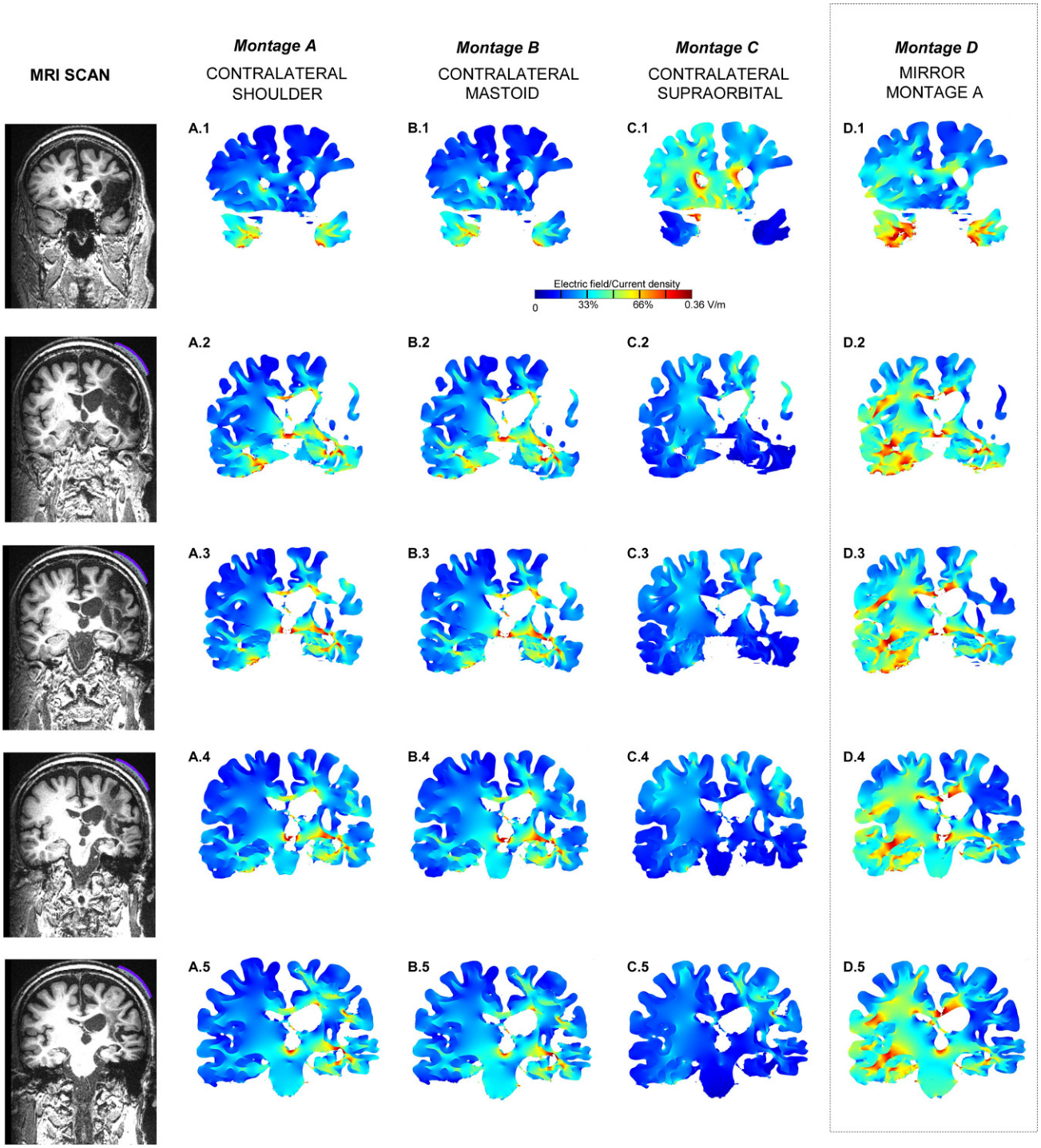

Figure 2 Cross-section cortical electric field plots of current flow for the different montages. All false color maps were generated between 0 and 0.36 V/m; the peak cortical EF magnitude for Montage A. First column: For all the plots, the corresponding coronal MRI scans collected for the subject is shown. The slices were chosen to highlight cross-sectional current flow in the *lesional* and *posterior perilesional* areas. Second column: Right shoulder; third column: right mastoid; fourth column: right orbitofrontal; fifth column: mirror Montage A.

recovery. Regardless of the conceptual treatment strategy, it is critical to know the resulting brain current flow for a given montage—and because of this complexity, requires individualized high-resolution modeling, as shown in this study. Indeed, these models thus provide a needed substrate to distinguish between therapeutic hypotheses precisely because simplistic and nonindividualized conceptions about brain current flow are insufficient.

Specifically, without models such as the one presented in this study, it will be difficult to understand the importance

of electrode placement on tDCS treatment outcome. For example, we have shown before that aphasia treatment success in stroke patients is supported by left-hemisphere brain plasticity.[13] If tDCS can be used to enhance brain plasticity in the left hemisphere, then it will be crucial to ensure that greatest stimulation occurs in left hemisphere regions. It is noteworthy that Montage A that produced significant benefit for the case–study subject also produced maximal stimulation of the posterior perilesional cortex, which was precisely the region of interest identified through fMRI analysis before therapy. Naturally, future research will have to adjudicate whether detailed, patient-specific electrode placement is crucial for tDCS benefit or if the same electrode placement can be applied to all patients, regardless of lesion location. We are currently working to solve this issue.

The tools developed for this case report represent an important advancement in high-resolution individualized modeling. The high spatial resolution makes it possible to resolve/segment thin structures more accurately that in turn leads to more precise/accurate—and hence individualized—3-dimensional rendering. An accurate 3-dimensional model allows for the precise computation of current flow and evaluation of individual factors, especially defects[11] and lesions. Preservation of 1 mm resolution in our models, led to several features being accurately captured (e.g., true lesion borders, cortical folds, zygomatic arch/process, foramen magnum, contiguous CSF layer, and ventricular architecture). For example, the general position of the lesion resulted in distinct brain-wide current flow distortion for each montage. On a still finer level, the precise representation of the perilesional region revealed detailed, but pronounced, differences across montages.

Continued technical improvements are indicated. Namely, further automation of the modeling process (critical for economical and broad dissemination) and additional sophistication in the imaging and modeling tissue properties around lesions is needed. Ultimately, neural activation is predicted by directly coupling field data to multicompartment biophysical models of individual neurons.[20] However it becomes unfeasible to incorporate neuron models of the entire cortex (with multiple different classes of neurons) in a macroscopic model presented in this study. Conversely, even as we demonstrate the value of precise and individualized anatomic representation, the use of generic and simplified geometries in (a) spheres[14,21] and (b) idealized lesions/defects[7,11] will continue to inform overall approaches to montage design.

In closing, the accuracy of predictions using forward models is limited by the precise representation of anatomy. Our development of high-resolution individualized models is thus an important advancement toward the use of computer models to retrospectively analyze results and prospectively design optimal electrotherapies.

References

1. Nitsche MA, Paulus W. Excitability changes induced in the human motor cortex by weak transcranial direct current stimulation. J Physiol 2000;527:633-639.
2. Iyer MB, Mattu U, Grafman J, et al. Safety and cognitive effect of frontal DC brain polarization in healthy individuals. Neurology 2005;64:872-875.
3. Sparing R, Dafotakis M, Meister IG, Thirugnanasambandam N, Fink GR. Enhancing language performance with non-invasive brain stimulation—a transcranial direct current stimulation study in healthy humans. Neuropsychologia 2008;46:261-268.
4. Hummel F, Cohen LG. Improvement of motor function with noninvasive cortical stimulation in a patient with chronic stroke. Neurorehabil Neural Repair 2005;19:14-19.
5. Baker JM, Rorden C, Fridriksson J. Using transcranial direct-current stimulation to treat stroke patients with aphasia. Stroke 2010;41:1229-1236.
6. Sunderam S, Gluckman B, Reato D, Bikson M. Toward rational design of electrical stimulation strategies for epilepsy control. Epilepsy Behav 2010;17:6-22.
7. Wagner T, Fregni F, Fecteau S, et al. Transcranial direct current stimulation: a computer based human model study. Neuroimage 2007;35:1113-1124.
8. Kertesz A. Western Aphasia Battery-Revised. San Antonio, TX: Harcourt Assessment, Inc; 2007.
9. Smith SM. Fast robust automated brain extraction. Human Brain Mapping 2002;17:143-155.
10. Jacobs MA, Zhang ZG, Knight RA, et al. A model for multiparametric MRI tissue characterization in experimental cerebral ischemia with histological validation in rat: part I. Stroke 2001;32:943-949.
11. Datta A, Bikson M, Fregni F. Transcranial direct current stimulation in patients with skull defects and skull plates: high-resolution computational FEM study of factors altering cortical current flow. Neuroimage 2010;52:1268-1278.
12. Datta A, Bansal V, Diaz J, et al. Gyri–precise head model of transcranial DC stimulation: improved spatial focality using a ring electrode versus conventional rectangular pad. Brain Stimul 2009;2:201-207.
13. Fridriksson J, Bonilha L, Baker JM, Moser D, Rorden C. Activity in preserved left hemisphere regions predicts anomia severity in aphasia. Cereb Cortex 2010;20:1013-1019.
14. Datta A, Elwassif M, Battaglia F, Bikson M. Transcranial current stimulation focality using disc and ring electrode configurations: FEM analysis. J Nerual Eng 2008;5:163-174.
15. De Lucia M, Parker GJ, Embleton K, Newton JM, Walsh V. Diffusion tensor MRI-based estimation of the influence of brain tissue anisotropy on the effects of transcranial magnetic stimulation. Neuroimage 2007;36:1159-1170.
16. Sadleir RJ, Vannorsdall TD, Schretlen DJ, Gordon B. Transcranial direct current stimulation (tDCS) in a realistic head model. Neuroimage 2010;51:1310-1318.
17. Jefferys JGR. Influence of electric fields on the excitability of granule cells in guinea-pig hippocampal slices. J Physiol 1981;319:143-152.
18. Bikson M, Inoue M, Akiyama H, et al. Effects of uniform extracellular DC electric fields on excitability in rat hippocampal slices in vitro. J Physiol 2004;557:175-190.
19. Bikson M, Datta A, Rahman A, Scaturro J. Electrode montages for tDCS and weak transcranial electrical stimulation: role of "return" electrode's position and size. Clin Neurophysiol 2010;121:1976-1979.
20. Butson CR, Cooper SE, Henderson JM, McIntyre CC. Patient-specific analysis of the volume of tissue activated during deep brain stimulation. Neuroimage 2007;34:661-670.
21. Miranda PC, Lomarev M, Hallett M. Modeling the current distribution during transcranial direct current stimulation. Clin Neurophysiol 2006;117:1623-1629.